American Journal of Mechanical Engineering and Automation
2019; 6(1): 1-8
http://www.openscienceonline.com/journal/ajmea
ISSN: 2381-6198 (Print); ISSN: 2381-6201 (Online)

Open Science

Implementation of Proportional-Integral-Plus Controller in Vehicle Active Suspension System

Hassan Metered[1, *], Abdelfattah Abdelhamid[2], Mohamed Abd Elhafiz[1]

[1]Automotive and Tractors Engineering Department, Faculty of Engineering, Helwan University, Cairo, Egypt

[2]Design Engineering Department, Faculty of Engineering, Helwan University, Cairo, Egypt

Email address

Hassan.metered@m-eng.helwan.edu.eg (H. Metered), Abdelfatah@m-eng.helwan.edu.eg (A. Abdelhamid), dr.mohamed.hafiz@m-eng.helwan.edu.eg (M. A. Elhafiz)

[*]Corresponding author

To cite this article

Hassan Metered, Abdelfattah Abdelhamid, Mohamed Abd Elhafiz. Implementation of Proportional-Integral-Plus Controller in Vehicle Active Suspension System. *American Journal of Mechanical Engineering and Automation*. Vol. 6, No. 1, 2019, pp. 1-8.

Received: March 10, 2019; **Accepted**: April 22, 2019; **Published**: May 9, 2019

Abstract

Proportional-integral-plus (PIP) controllers are simple, effective in dealing with nonlinearities and offering a rational extension of traditional proportional-integral/proportional-integral-derivative (PI/PID) techniques, with extra dynamic feedback and input compensators introduced automatically specially when the system is complicated or has considerable time delays. This paper investigates the implementation of a PIP controller based on a non-minimal state space (NMSS) form in a vehicle active suspension system, for the first time, to enhance ride comfort and vehicle stability. The active vehicle suspension system is modeled as a two degrees–of–freedom mechanical system and simulated using Matlab/Simulink software. The performance of the proposed vehicle active suspension system controlled using the PIP is compared to active suspension controlled using proportional-integral-derivative (PID) controller and passive suspension systems. Systems performance criteria are evaluated in time and frequency domains to assess the efficiency of the proposed PIP controller. Theoretical results confirm that the proposed PIP controller of vehicle active suspension system grants a significant enhancement of ride comfort and vehicle stability.

Keywords

Active Vehicle Suspension System, Quarter Car Model, Proportional-Integral-Plus (PIP) Controller, PID

1. Introduction

The PIP controller can be considered as a logical extension of conventional PI/PID controllers. It has a dynamic feedback and input compensators used automatically when the plant contains higher dynamics and/or time delays [1]. However, PIP technique has various advantages: in particular, its structure exploits the power of state variable feedback methods, where the vagaries of manual tuning are replaced by pole assignment or Linear Quadratic (LQ) design. Tuning of PID controllers has still been a critical problem because many industrial models are often restricted with characteristics such as higher order, time delay and nonlinearities [2, 3], which could lead to overshoot, cyclic/slow response, poor robustness and collapse the whole system [4]. Nevertheless, PIP controller uses extra output gains to counter the influence of higher order models, also exploiting extra input gains to counteract the influence of time delay models.

The design of good quality control algorithms for active vehicle suspensions is a key issue for the vehicle industry. A good suspension system should improve ride quality and road holding/vehicle stability. In order to improve ride quality, it should drop the vertical body acceleration of the vehicle body due to unwanted disturbances of the road surface. In terms of road holding, it should offer an adequate tyre-terrain contact and drop the dynamic tyre deflection. So, good quality suspension systems are tough to obtain because they contain a trade-off between ride quality and vehicle stability [5].

Suspension systems are categorized into three major

classes; passive, active and semi-active [6]. Passive suspensions are simple, cheap and reliable. Active and semi-active suspensions have control units which perform the performance of some reference and optimized systems. Active suspensions incorporate active devices such as electro-hydraulic actuators which can be ordered in a direct way to generate a controlled damping force. Semi-active suspensions employ semi-active damper whose force is ordered indirectly through a change in the dampers' properties.

Active suspensions can offer superior performance over a wide range of frequency compared with passive suspensions [7, 8]. Immediately, control algorithms of active suspensions have been proposed from a principally linear quadratic regulator (LQR) to smart and intelligent controllers depend on modern outcomes of computational intelligence.

Several investigations have been done on the implementations of advanced control techniques to improve the performance of active suspensions during the last three decades. For example, optimal control [9], model reference adaptive control [10], adaptive control [11, 12], H∞ [13], LQG control [14], sliding mode control strategy [15, 16], fuzzy logic control [17], and self-tuning PID controller [18], optimized fuzzy-PID [19] and the references therein, have been applied in active systems.

The novel contribution of this paper is the implementation of PIP controller based on a non-minimal state space (NMSS) form in vehicle active suspension system, for the first time. Control performance criteria are evaluated in both time and frequency domains in order to judge the active suspension success controlled using PID and PIP compared to passive suspension system. The rest of this article is organized as follows: an overview of the quarter vehicle model is introduced in section (2). Section (3) introduces a description of the proposed control algorithms focusing PIP algorithm. The results obtained for different road disturbance inputs are presented and discussed in section (4). Finally, section (5) summarizes the conclusion.

2. Quarter Vehicle Model

Figure 1 shows a two-degrees-of-freedom (2-DOF) mechanical system that symbolizes an actively quarter vehicle suspension model. It consists of sprung and un-sprung masses; m_b represents the body mass, sprung mass, and m_w represents the wheel mass, un-sprung mass, and its linked parts. The vertical motion of the quarter vehicle suspension system is described by the displacements x_b and x_w while the road disturbance is x_r. k_s is the suspension spring stiffness and k_t is the tyre spring stiffness. The tyre damping coefficient can be neglected due to its very small value. The data used in this paper for the quarter vehicle model is selected from ref. [20] and listed in Table 1. Newton's second law is applied to the quarter vehicle suspension model to derive equations of motion of m_b and m_w as follows:

$$\begin{aligned} m_b\ddot{x}_b + k_s(x_b - x_w) + c_s(\dot{x}_b - \dot{x}_w) + f_a = 0 \\ m_w\ddot{x}_w - k_s(x_b - x_w) - c_s(\dot{x}_b - \dot{x}_w) + k_t(x_w - x_r) - f_a = 0 \end{aligned} \quad (1)$$

State space representation is done to represent the proposed active suspension system in the following form:

$$\dot{x} = A\,x + B\,f_a + D\,x_r \quad (2)$$

Where, $x = [x_b \;\; x_w \;\; \dot{x}_b \;\; \dot{x}_w]^T$,

$$A = \begin{bmatrix} 0 & 0 & 1 & 0 \\ 0 & 0 & 0 & 1 \\ -\frac{k_s}{m_b} & \frac{k_s}{m_b} & -\frac{c_s}{m_b} & \frac{c_s}{m_b} \\ \frac{k_s}{m_w} & -\frac{k_s + k_t}{m_w} & \frac{c_s}{m_w} & -\frac{c_s}{m_w} \end{bmatrix}$$

$$B = \begin{bmatrix} 0 & 0 & -\frac{1}{m_b} & \frac{1}{m_w} \end{bmatrix}^T, \text{ and } D = \begin{bmatrix} 0 & 0 & 0 & \frac{k_t}{m_w} \end{bmatrix}^T$$

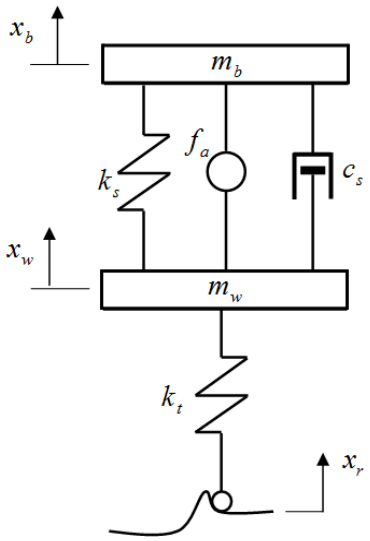

Figure 1. *Quarter-vehicle active suspension model.*

Table 1. *Quarter vehicle suspension parameters [20].*

Parameter	Symbol	Value (Unit)
Body Mass Mass of vehicle wheel Suspension stiffness Damping coefficient Tyre stiffness	m_b	375 (kg)
Wheel Mass	m_w	29.5 (kg)
Suspension stiffness	k_s	20.58 (kN/m)
Damping coefficient	c_s	772 (Ns/m)
Tyre stiffness	k_t	200 (kN/m)

For controlled active suspension systems, the actuator force f_a is calculated based on the time history of the relative displacement between sprung and un-sprung masses which known as suspension working space (SWS).

3. Active Control Algorithms

This section offers an overview of the applied active control algorithms in this paper, which are mainly a PID controller based on mathematical calculations of Ziegler–Nichols closed loop method and PIP controller based on a Non-minimal State Space (NMSS) form.

3.1. PID Controller

PID controller consists of three gains only; proportional, integral and derivative as shown in Figure 2. The controller force f_a is determined by

$$f_a = k_p e + k_i \int e dt + k_d \frac{de}{dt} = u(t) \tag{3}$$

$$e = x_b - x_w \equiv SWS \tag{4}$$

where $e(t)$ is the control error, $r(t)$ is the reference relative displacement between body and wheel masses, known as SWS, assumed to be zero. K_p is the proportional gain, K_i the integral gain and K_d the derivative gain.

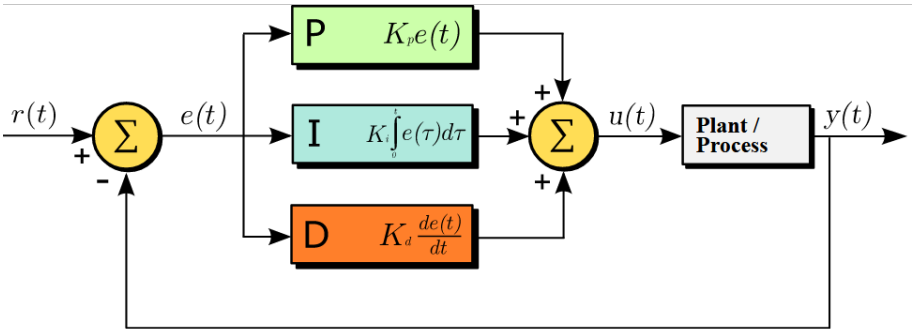

Figure 2. *The Basic construction of the PID controller.*

The gains K_p, K_i and K_d of the PID controller are computed based on Ziegler–Nichols closed loop method [21] and set to K_p=5640, K_i = 3807 , and K_d=2920.

3.2. PIP Controller

Once the discrete-time TF is identified and estimated, it is easy to show that this model can be represented in the following NMSS form:

$$\begin{aligned} \boldsymbol{x}_k &= \boldsymbol{F}\, x_{k-1} + \boldsymbol{g}\, u_{k-1} + \boldsymbol{d}\, r_k \\ y_k &= \boldsymbol{h}\, \boldsymbol{x}_k \end{aligned} \tag{5}$$

for which $\boldsymbol{x}_k = [y_k \ \cdots \ y_{k-n+1} \ u_{k-1} \ \cdots \ u_{k-m+1} \ z_k]^T$ is the n+m dimensional state vector, consisting of the present and past values of the output variable y_k and the past values of the input u_k. With this special NMSS representation, all the states are directly measurable. Moreover, the NMSS description includes the following integral-of-error state z_k to ensure tracking performance

$$z_k = z_{k-1} + (r_k - y_k) \tag{6}$$

for which r_k is the reference or command input. Finally, the state transient matrix F, input vector g, command input vector d and output vector h are defined as follows,

$$\boldsymbol{F} = \begin{bmatrix} -a_1 & -a_2 & \cdots & -a_{n-1} & -a_n & b_2 & b_3 & \cdots & b_{m-1} & b_m & 0 \\ 1 & 0 & \cdots & 0 & 0 & 0 & 0 & \cdots & 0 & 0 & 0 \\ 0 & 1 & \cdots & 0 & 0 & 0 & 0 & \cdots & 0 & 0 & 0 \\ \vdots & \vdots & \ddots & \vdots & \vdots & \vdots & \vdots & \ddots & \vdots & \vdots & \vdots \\ 0 & 0 & \cdots & 1 & 0 & 0 & 0 & \cdots & 0 & 0 & 0 \\ 0 & 0 & \cdots & 0 & 0 & 0 & 0 & \cdots & 0 & 0 & 0 \\ 0 & 0 & \cdots & 0 & 0 & 1 & 0 & \cdots & 0 & 0 & 0 \\ 0 & 0 & \cdots & 0 & 0 & 0 & 1 & \cdots & 0 & 0 & 0 \\ \vdots & \vdots & \ddots & \vdots & \vdots & \vdots & \vdots & \ddots & \vdots & \vdots & \vdots \\ 0 & 0 & \cdots & 0 & 0 & 0 & 0 & \cdots & 1 & 0 & 0 \\ a_1 & a_2 & \cdots & a_{n-1} & a_n & -b_2 & -b_3 & \cdots & -b_{m-1} & -b_m & 1 \end{bmatrix} \tag{7}$$

$$\boldsymbol{g} = [b_1 \ 0 \ \cdots \ 0 \ 1 \ 0 \ 0 \ \cdots \ 0 \ 0 \ -b_1]^T$$

$$\boldsymbol{d} = [0 \ 0 \ \cdots \ 0 \ 0 \ 0 \ 0 \ \cdots \ 0 \ 0 \ 1]^T$$

$$\boldsymbol{h} = [1 \ 0 \ \cdots \ 0 \ 0 \ 0 \ 0 \ \cdots \ 0 \ 0 \ 0]$$

The state variable feedback (SVF) control law associated with the NMSS model represented in equation (1) then takes the form,

$$u_k = -\boldsymbol{k}\,\boldsymbol{x}_k \tag{8}$$

where k is the $n+m$ dimensional SVF control gain vector,

$$\boldsymbol{k} = [f_o \;\; f_1 \;\; \cdots \;\; f_{n-2} \;\; f_{n-1} \;\; g_1 \;\; g_2 \;\; \cdots \;\; g_{m-2} \;\; g_{m-1} \;\; -k_I]^T \tag{9}$$

This SVF control gain vector not only contains proportional and integral gains, like a PI controller, but also includes higher order input and output feedback compensators which enhance the performance of the controller as depicted in Figure 3 below. As shown in this figure, PIP control can be considered as an extension of PI control, for which the PI action is enhanced by the higher order input and output feedback compensators $G_1(z^{-1})$ and $F_1(z^{-1})$ respectively, where

$$\begin{aligned} G_1(z^{-1}) &= g_1 z^{-1} + g_2 z^{-2} + \cdots g_{m-1} z^{-(m-1)} \\ F_1(z^{-1}) &= f_1 z^{-1} + f_2 z^{-2} + \cdots + f_{n-1} z^{-(n-1)} \end{aligned} \tag{10}$$

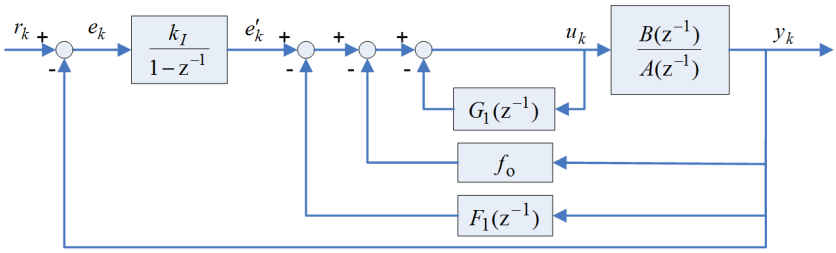

Figure 3. *The PIP control system implemented in standard feedback form.*

Since all the state variables in $\boldsymbol{x}_k$ are readily stored in the digital computer, the PIP controller can be implemented easily. Moreover, the inherent SVF formulation allows for the exploitation of any SVF procedure such as optimisation in terms of Linear Quadratic LQ cost function.

In the case of optimization in terms of a Linear Quadratic LQ cost function, the SVF gain vector can be obtained that satisfies predetermined conditions or weighting criteria. The problem of optimization could be defined as follows: for a linear SISO discrete NMSS form defined in equation (5), it is required to find the control law in equation (8) with optimal SVF control gain vector that minimizes the following quadratic cost function,

$$J = \sum_{i=0}^{\infty} \left\{ \boldsymbol{x}_i^T \boldsymbol{Q}\, \boldsymbol{x}_i + R\, u_i^2 \right\} \tag{11}$$

where Q is a square positive definite matrix with dimension $n+m$, which is defined as follows,

$$\boldsymbol{Q} = diag\left[q_{y_1} \;\; \ldots\ldots \;\; q_{y_n} \;\; q_{u_1} \;\; \ldots\ldots \;\; q_{u_m} \;\; q_e\right] \tag{12}$$

and R is an additional scalar weight on the input. Here, q_{y_i} ($i = 1, 2, \cdots, n$) are the output weighting parameters, q_{u_j} ($j = 1, 2, \cdots, m$) are the input weighting parameters and q_e provides the weighting on the integral of error state variable z_k.

The resulting SVF gains are then obtained recursively from the steady state solution of the Algebraic Riccati Equation (ARE) [22], derived from the standard LQ cost function in equation (11) as follows,

$$\begin{aligned} \boldsymbol{k} &= \left[\boldsymbol{g}^T \boldsymbol{P}^{(i+1)} \boldsymbol{g} + R\right]^{-1} \boldsymbol{g}^T \boldsymbol{P}^{(i+1)} \boldsymbol{F} \\ \boldsymbol{P}^{(i)} &= \boldsymbol{F}^T \boldsymbol{P}^{(i+1)} \left[\boldsymbol{F} - \boldsymbol{g}\,\boldsymbol{k}\right] + \boldsymbol{Q} \end{aligned} \tag{13}$$

for which $\boldsymbol{P}$ is a symmetrical positive-definite matrix with the initial value, $\boldsymbol{P}^{(i+1)}$, equal to the weighting matrix $\boldsymbol{Q}$ and $\boldsymbol{k}$ is the control gain vector.

4. Results and Discussion

In this section, the efficiency of applied control algorithms for an actively vehicle suspension system is investigated through numerical simulations under two types of road excitations. There are three main performance criteria in vehicle suspension design that assess ride comfort and vehicle stability; suspension working space (*SWS*), vertical body acceleration (*BA*), and dynamic tyre load (*DTL*). The performance criteria are evaluated in both time and frequency domains to assess ride comfort and vehicle stability. Ride comfort is related to the *BA*. To certify good vehicle stability, it is required that the tyre's dynamic deflection $(x_w - x_r)$ should be low [23]. The structural appearances of the vehicle also constrain the amount of *SWS* within acceptable certain limits. The goal is to minimize *SWS*, *BA*, and *DTL* in order to improve suspension performance.

The numerical results are demonstrated in this section for three types of suspension systems: (a) passive suspension, (b)

active suspension controlled using PID controller and (c) active suspension controlled using PIP controller.

The aforementioned performance criteria are studied to quantify the relative performance of these control methods. Since the passive vehicle suspension system is used as a base-line for comparisons. Two road excitations are chosen to be very similar to the real-world road profiles; the first excitation normally used to reflect the transient response is a road bump which described by [24] as:

$$x_r = \begin{cases} a\ \{1-\cos(\omega_r(t-0.5))\}, & \text{for} \quad 0.5 \le t \le 0.5+\dfrac{d_b}{V_c} \\ 0, & \text{otherwise} \end{cases} \quad (14)$$

where a is the half of the bump amplitude, $\omega_r = 2\pi V_c / d_b$, d_b is the bump width and V_c is the vehicle velocity. In this study $a = 0.035$ m, $d_b = 0.8$ m, $V_c = 0.856$ m/s, as in [24].

The time history of the suspension system response under bumpy road disturbance is shown in Figure 4. The displacement of the road input signal is shown in Figure 4 (a) and the *SWS*, *BA*, and *DTL* responses are presented in Figures 4 (b, c, and d), respectively. The latter figures show the comparison between the controlled active using PID, PIP controllers, and passive suspension systems. From these results, it is clearly seen that the PIP controlled suspension system can dissipate the energy due to bump excitation very well, cut down the settling time, and improve both the ride comfort and vehicle stability.

The peak-to-peak (PTP) values of the system response are summarized in Table 2, which shows that the two controlled systems have the lowest peaks for the *SWS*, *BA*, and *DTL*, demonstrating their effectiveness at improving the ride comfort and vehicle stability. The controlled system using PIP controller can reduce maximum peak-to-peak of *SWS*, *BA*, and *DTL* by 36.7%, 13.8% and 12.3%, respectively, compared with the controlled system using PID controller. Also, the two active suspension systems were compared with the conventional passive system and the improvement percentages are listed in Table 2. The results illustrate that the active vehicle suspension system controlled using PIP offers a good performance.

The second type of road excitation was a random road profile described by [24] as:

$$\dot{x}_r + \rho V x_r = V W_n \quad (15)$$

where W_n is white noise with intensity $2\sigma^2 \rho V$, ρ is the road irregularity parameter, and σ^2 is the covariance of road irregularity. In random road excitation, the values of road surface irregularity (ρ =0.45 m^{-1} and σ^2 =300 mm^2) were selected assuming that the vehicle moves on the paved road with the constant speed V = 20 m/s, as in [24].

In order to enhance ride comfort, it is significant to isolate the vehicle body from road disturbances and to drop the resonance peak of the body mass near 1 Hz which is recognized to be a sensitive frequency to the human body [23, 25]. Additionally, in order to enhance vehicle stability, it is significant to keep the tyre in contact with the road surface and therefore to drop the resonance peak near 10 Hz, which is the resonance frequency of the wheel [23, 25]. In view of these concerns, the results achieved for the excitation described by equation (15) are introduced in the frequency domain.

Figure 5 shows the modulus of the Fast Fourier Transform (FFT) of the *SWS*, *BA*, and *DTL* responses over the range 0.5-20 Hz. The FFT was properly scaled and smoothed by curve fitting as done in [26]. It is evident that the lowest resonance peaks for body and wheel can be achieved using the proposed PIP controller. According to these figures, just like for the bump excitation, the controlled system using PIP controller can dissipate the energy due to road excitation very well and enhance both ride comfort and vehicle stability.

In the case of random excitation, it is the root mean square (*RMS*) values of the *SWS*, *BA*, and *DTL*, instead of their peak-to-peak values that are relevant. These are illustrated in Table 3, which shows that the controlled system using PIP controller has the lowest levels of *RMS* values for the *SWS*, *BA*, and *DTL*. PID GA controller can reduce maximum *RMS* values of *SWS*, *BA*, and *DTL* by 29.3%, 17.2% and 5.9%, respectively, compared with the PID system. Table 3 also compares the two active suspension systems with the passive system. The results again confirm that the active vehicle suspension system controlled using PIP controller can give a good response in terms of ride comfort and vehicle stability.

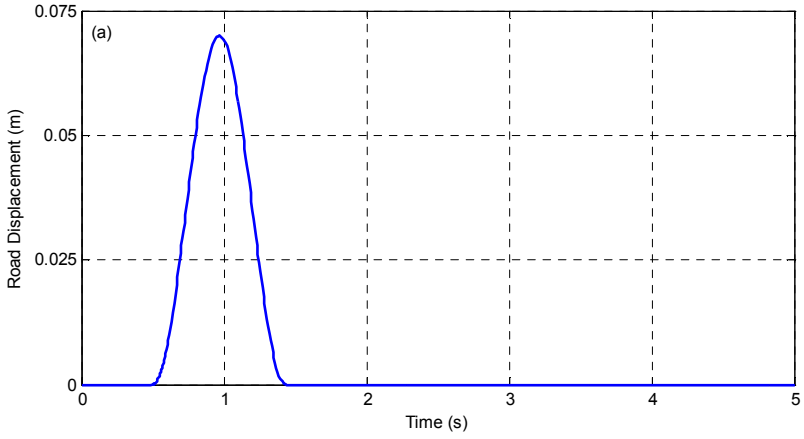

a. Road Displacement

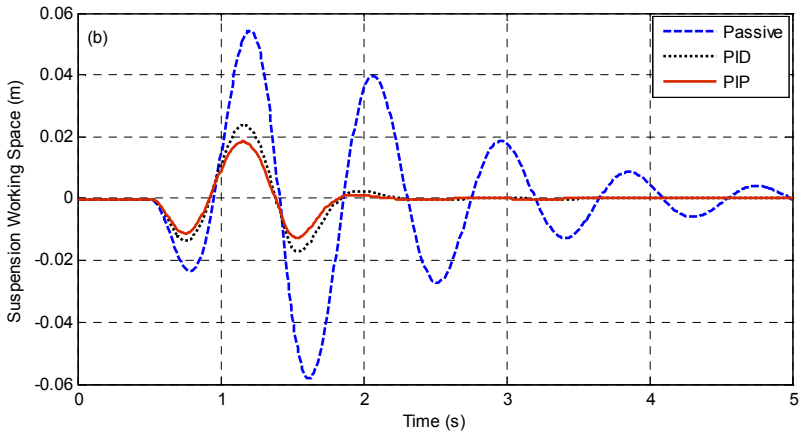

b. SWS

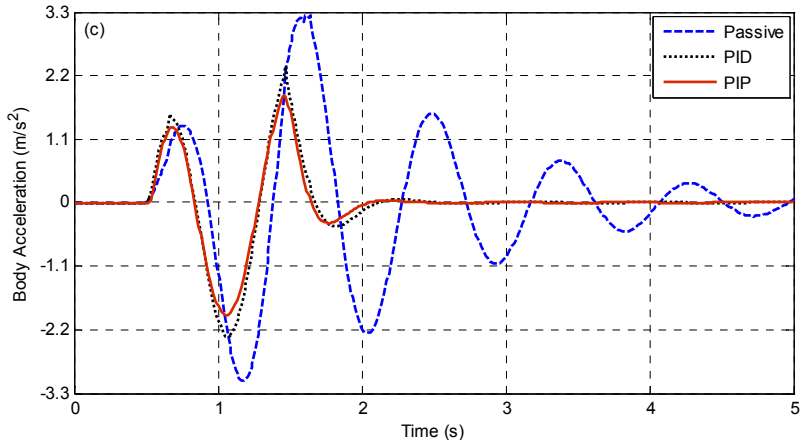

c. BA

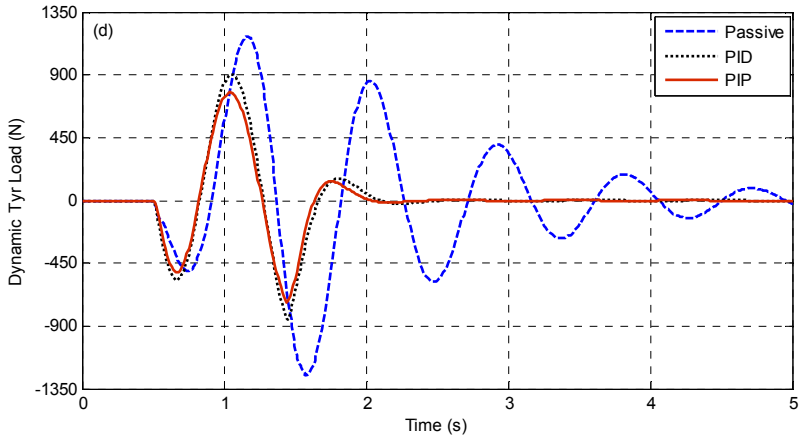

d. DTL

Figure 4. *The time history of system response under road bump excitation.*

Table 2. *PTP values and improvement ratios of road disturbance excitation.*

System Type	SWS (m)	% Imp. Respect to Passive	% Imp. Respect to PID	BA (m/sec^2)	% Imp. Respect to Passive	% Imp. Respect to PID	DTL (N)	% Imp. Respect to Passive	% Imp. Respect to PID
Passive	0.1125	-	-	6.38	-	-	2429	-	-
PID	0.049	56.5	-	4.42	30.7	-	1704	29.8	-
PIP	0.031	72.4	36.7	3.81	40.3	13.8	1495	38.5	12.3

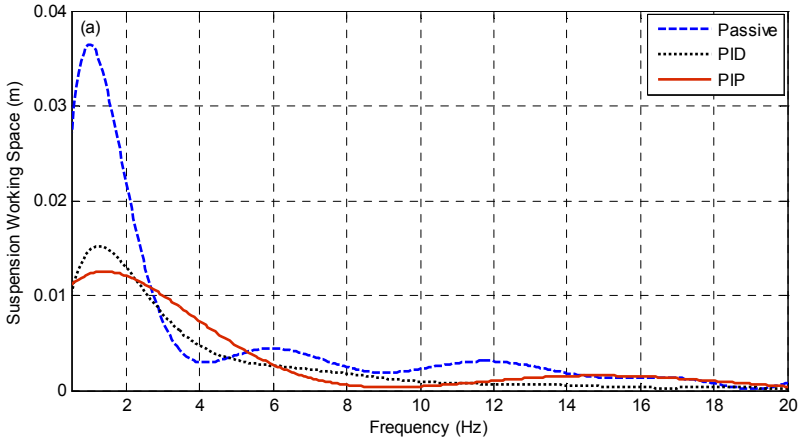

a. SWS

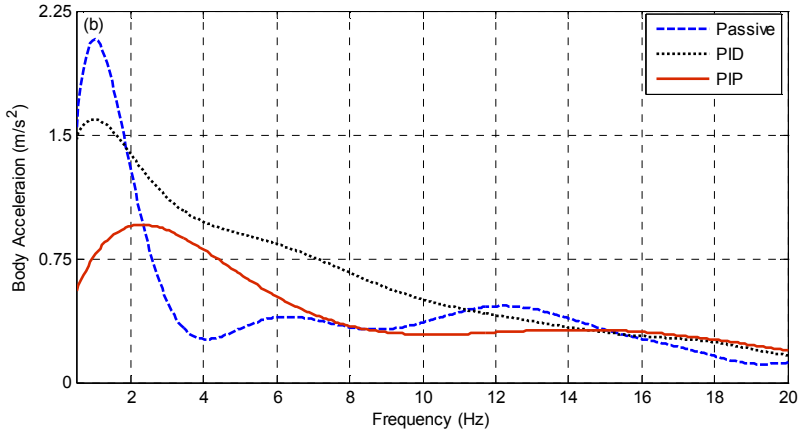

b. BA

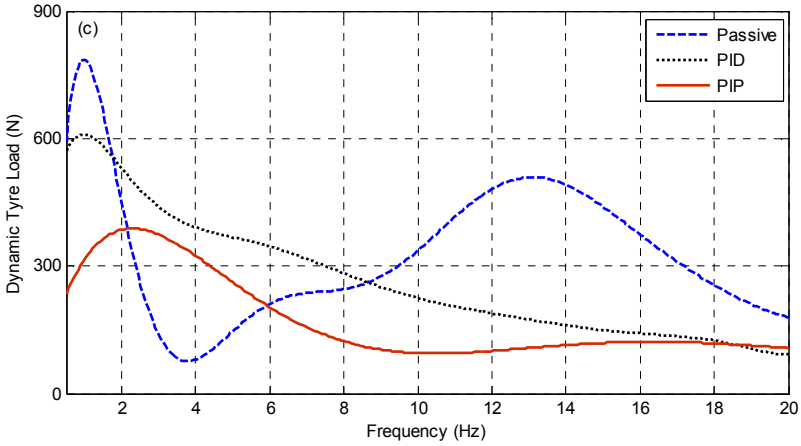

c. DTL

Figure 5. *The modulus of the Fast Fourier Transform.*

Table 3. *RMS values and improvement ratios of random road excitation.*

System Type	SWS (m)	% Imp. Respect to Passive	% Imp. Respect to PID	BA (m/sec^2)	% Imp. Respect to Passive	% Imp. Respect to PID	DTL (N)	% Imp. Respect to Passive	% Imp. Respect to PID
Passive	0.0152	-	-	1.43	-	-	592.5	-	-
PID	0.0075	50.6	-	0.99	30.8	-	438.8	25.7	-
PIP	0.0053	65.1	29.3	0.82	43.4	17.2	413	30.3	5.9

5. Conclusions

In this paper, a PIP controller based on a non-minimal state space (NMSS) form is applied in vehicle active suspension system, for the first time. A mathematical model of an active quarter-vehicle suspension system was derived and simulated using Matlab/Simulink software. The system performance generated by PIP controller is compared with PID controller tuned according to Ziegler–Nichols method and passive suspension systems. Systems performance criteria were evaluated in time and frequency domains in order to prove the introduced active suspension effectiveness under bump and random road excitations. As a final point, theoretical results showed that the PIP controller potentially enhance ride comfort and vehicle stability levels over the PID controller.

References

[1] Dixon, R., C. James Taylor, and E. M. Shaban. "Comparison of classical and modern control applied to an excavator arm." IFAC Control 2005, 4-8 July (2005).

[2] Shaban, E., H. Sayed, and A. Abdelhamid, “A novel discrete PID+ controller applied to higher order/time delayed nonlinear systems with practical implementation”. International Journal of Dynamics and Control, 2018: p. 1-13.

[3] Deepa SN, Sugumaran G. Design of PID controller for higher order continuous systems using MPSO based model formulation technique. International Journal of Electrical and Electronics Engineering. 2011 Aug 29; 5 (4): 289-95.

[4] Ali H, Wadhwani S. Intelligent PID controller tuning for higher order process system. International Journal of u-and e Service, Science and Technology. 2015; 8 (6): 323-330.

[5] Gillespie TD, Fundamentals of Vehicle Dynamics, SAE International: 1993.

[6] El-taweel H., Abd elhafiz M. M., and Metered H., Optimal lumped parameters estimation of vehicle passive suspension system using genetic algorithm, Journal of Advances in Vehicle Engineering, 2018, Vol. 5 No. 1, pp. 34-44.

[7] Cao, J. Li, P., and Liu, H., An interval fuzzy controller for vehicle active suspension systems. IEEE Transactions on Intelligent Transportation Systems: 11 (4), 885–895, 2010.

[8] Gao, H., Lam, J., and Wang, C., Multi-objective control of vehicle active suspension systems via load-dependent controllers, Journal of Sound and Vibration: 290 (3-5), 654–675, 2006.

[9] Hrovat, D., Survey of advanced suspension developments and related optimal control applications, Automatica: 33 (10), 1781–1817, 1997.

[10] Mohan, B., Modak, J. P., Phadke, S. B., Vibration control of vehicles using model reference adaptive variable structure control. Advances in Vibration Engineering: 2 (4), 343–361, 2003.

[11] Fialho, I., and Balas, J., Road adaptive active suspension design using linear parameter-varying gain-scheduling. IEEE Transactions on Control Systems Technology: 10 (1), 43–54, 2002.

[12] Rajamani, R., and Hedrick, J., Adaptive observers for active automotive suspensions: theory and experiment. IEEE Transactions on Control Systems Technology: 3 (1), 86–93, 1995.

[13] Gao, H., Sun, W., and Shi, P., Robust sampled-data H_∞ control for vehicle active suspension systems. IEEE Transactions on Control Systems Technology: 18 (1), 238–245, 2010.

[14] Metered H., Application of Nonparametric Magnetorheological Damper Model in Vehicle Semi-active Suspension System, SAE Int. J. Passeng. Cars - Mech. Syst: 5 (1), 2012.

[15] Metered H., and Šika Z., Vibration control of vehicle active suspension using sliding mode under parameters uncertainty, Journal of Traffic and Logistics Engineering: 3 (2), 2015.

[16] Vaijayanti, S. D., Mohan, B., Shendge, P. D., and Phadke S. B., Disturbance observer based sliding mode control of active suspension systems, Journal of Sound and Vibration: 333 (11), 2281–2296, 2014.

[17] Emam, A. S., Active Vibration Control of Automotive Suspension System using Fuzzy Logic Algorithm. Int. J. of Vehicle Structures & Systems: 9 (2), 77-82, 2017.

[18] Emam, A. S., Fuzzy Self Tuning of PID Controller for Active Suspension System, Advances in Powertrains and Automotive: 1 (1), 34-41, 2015.

[19] El-taweel H., Abd elhafiz M. M., and Metered H., Vibration control of active vehicle suspension system using optimized fuzzy-PID, SAE Technical Paper, 2018-01-1402, 2018.

[20] Choi, S. B., Choi, Y. T., and Park, D. W., A sliding mode control of a full-car electrorheological suspension system via hardware in-the-loop simulation, Dynamic Systems, Measurement, and Control: Volume: 122, pp 114-121, 2000.

[21] Michael, A. J., and Mohammad H. M., PID Control: New Identification and Design Methods, Springer-Verlag London Limited: 2005.

[22] Astrom, K. J. and Wittenmark, B., “Computer Controlled Systems: Theory and Design”. Prentice-Hall Information and System Sciences Series, 1984.

[23] Rajamani, R., Vehicle dynamics and control, Springer Science and Business Media: New York, 2006.

[24] Choi, S. B., and Kim, W. K., Vibration control of a semi-active suspension featuring electrorheological fluid dampers, Journal of Sound and Vibration: 234, 537-546, 2000.

[25] Fischer, D., and Isermann, R., Mechatronic semi-active and active vehicle suspensions, Control Engineering Practice: 12 (11): 1353-1367, 2004.

[26] Metered, H., Modelling and Control of Magnetorheological Dampers for Vehicle Suspension Systems, PhD Thesis, School of Mechanical, Aerospace and Civil Engineering, The University of Manchester: Manchester, UK. 2010.